Above-Threshold Leakage in Semiconductor Lasers: An Analytical Physical Model

Igor M. P. Aarts and Edward H. Sargent

***Abstract*—We present an analytical physical model for above-threshold leakage in semiconductor lasers. The model can be applied to estimate whether heterobarrier lowering and accompanying overbarrier leakage are within reach of having serious deleterious effects on laser performance. The model uses two-dimensional fully self-consistent numerical equations that arise from comprehensive systems of partial coupled differential equations. The effect of temperature and doping on laser efficiency is analyzed for two lasers, one designed for operation at 1.3 μm and the other at 1.55 μm. Both devices are assumed to be built in the InGaAsP-InP material system. We show that, even in a 1.55-μm laser, overbarrier leakage can cause severe performance degradation at typical operating temperatures and doping levels, and we argue that overbarrier leakage deserves to be treated as a potential threat to laser performance at telecommunication wavelengths.**

***Index Terms*—Analytical model, doping, internal efficiency, overbarrier leakage, semiconductor laser, telecommunication, temperature.**

I. Introduction

THE above-threshold efficiency of semiconductor lasers emitting light at 1.3 μm and 1.55 μm has attracted significant attention over the past twenty years. The use of lasers in CATV distribution systems and in emerging metropolitan-area networks further exacerbates the need for efficient operation of uncooled lasers. By eliminating the need for active cooling, the development of uncooled lasers achieves cost reduction, low power consumption, and compactness [1].

Westbrook and Nelson [2] proposed an analytical model for electron leakage in 1.5-μm separate-confinement heterostructure lasers but neglect the role of leakage of active region carriers over the heterobarrier into the minority contact (overbarrier leakage). Kazarinov and Pinto [3] quantified explicitly the role of overbarrier leakage in double-heterostructure semiconductor lasers. They explored the role of injected forward current in lowering the confinement barrier for the electrons. In their model, the authors considered simultaneously Poissons's equation, current continuity for electrons and holes, drift and diffusion, Auger recombination, Shockley–Read–Hall recombination, and spontaneous and stimulated emission terms. They explored the role of forward current and temperature on thermionic emission of electrons from the active region and, consequently, on internal quantum efficiency.

Manuscript received August 5, 1999; revised November 18, 1999.

The authors are with the Physics Department, Eindhoven University of Technology, 5600 MB Eindhoven, The Netherlands.

Publisher Item Identifier S 0018-9197(00)02699-3.

If the mechanism of heterobarrier lowering using fully self-consistent numerical simulation [3], [4] and reported experimentally in [5] can, indeed, represent a significant cause of efficiency degradation, then the laser designer will benefit greatly by having a simplified, direct, analytical model, and correspondingly straightforward physical understanding of this effect. Before proceeding to obtain two-dimensional (2-D) fully self-consistent numerical solutions to the comprehensive system of coupled partial differential equations, a simplified model could be applied to estimate whether heterobarrier lowering and accompanying overbarrier leakage are indeed within reach of having serious deleterious effects on laser performance.

II. Model

We seek in this work to consider the role of overbarrier leakage in isolation from all other mechanisms potentially responsible for above-threshold efficiency degradation. Such other effects include parallel leakage, injection-level-dependent free carrier absorption, and Auger recombination and associated carrier heating. We take each of these effects to be a parameter in our model. Thus, full consideration of all such mechanisms combined is readily achieved by parameterizing each according to its dependencies on structure and bias. In this work, we consider instead the direct impact of overbarrier leakage on efficiency degradation assuming that all other efficiency-degrading mechanisms remain fixed above the lasing threshold.

We begin with [3, eq. (4)]

$$q\Delta V = kT \ln\left(1 + \frac{J_{\mathrm{act}} L_D \exp\left(\dfrac{\Delta E_V - \Delta E_{Fn} - \Delta E_{Fp}}{kT}\right)}{\sqrt{2}\mu_p N_A \sqrt{qV_1 kT}}\right). \tag{1}$$

The meaning of each symbol is explained in Table I and illustrated in Fig. 1. In this work, except when stated otherwise, we use the material parameters given in Table I, obtained from [6], for bulk lasers operating at 1.3 μm.

The effects explored in this work are important in both bulk and quantum-well (QW) lasers. In the quantitative portions of this work, we consider for illustrative purposes the case of bulk lasers. This approach applies to the case of overbarrier leakage from the (bulk) separate-confinement heterostructure (SCH) region of a QW laser as well. To consider leakage directly from

TABLE I
MATERIAL PARAMETERS

	Parameter	Value	
		1.3 μm	1.55 μm
q	electron charge	1.6×10^{-19} C	
k	Boltzmann's constant	1.38×10^{-23} J/K	
T	temperature	300 K	
μ_p	hole mobility (at 300 K)	200 cm^2/Vs	
μ_n	electron mobility (at 300 K)	3000 cm^2/Vs	
n_{act}	electron density in active region	2×10^{24} m^{-3}	
τ_n	electron lifetime in p-contact	10^{-9} s	
N_A	acceptor concentration in depletion layer	4×10^{17} cm^{-3}	
σ_p	electrical conductivity of the p-cladding layer	$qN_A\mu_p$	
L_D	extrinsic Debye length	$\sqrt{\frac{kT\varepsilon}{4\pi N_A q^2}}$	
D_n	diffusion coefficient	$\frac{\mu_n kT}{q}$	
L_n	electron diffusion length	$\sqrt{D_n\tau_n}$	
L_{nf}	electron drift length	$2\left(\frac{kT}{q}\right)\frac{\sigma_p}{J_{act}}$	
ΔE_V	discontinuity of the valence band	0.24 eV	0.317 eV
ΔE_{Fn}	difference between conduction band edge and electron Fermi level energy	$\approx kT$	$\approx kT$
ΔE_{Fp}	difference between valence band edge and hole Fermi level energy	$\approx kT$	$\approx kT$
$q\Delta V$	change in hole quasi-Fermi level at heterojunction		
V_l	potential drop in depletion layer		

QW states to a bulk material, it is necessary to modify the effective density of states used in the relation between carrier density and quasi-Fermi energy.

As explained in [3], the quantity V_1 represents the potential drop in the depletion layer. This quantity is in turn related to the properties of the heterostructure at equilibrium and to the degree of forward injections:

$$V_1 = V_{\rm bi} - V_{\rm act} = V_{\rm bi} - (V_{qf} + \Delta V) \tag{2}$$

where $V_{\rm bi}$ represents the built-in voltage at zero bias, V_{qf} represents the bias required to separate the quasi-Fermi levels inside the active region (a quantity which is very well approximated by a constant value above the lasing threshold), and ΔV takes on the same meaning as in (1).

Upon substitution of (2) into (1), it is clear that the solution for the extent of heterobarrier lowering for a given forward current density J must be found using iterative methods. However, for small ΔV relative to $V_{\rm bi} - V_{qf}$, the rate of change of the right-hand side of (1) with ΔV is small compared to the rate of change of the left-hand side. It may be seen from Fig. 2 that, over a broad range of parameters, the solution for ΔV from (1) is approximated well by neglecting its influence on V_1.

As a further simplification, the behavior of (1) may be subdivided into two regimes: one which is linear in J and another which is logarithmic in J. For current densities less than

$$J_{\rm transition} = \frac{\sqrt{2}\mu_p N_A\sqrt{qV_1kT}}{L_D\exp\left(\dfrac{\Delta E_V - \Delta E_{Fn} - \Delta E_{Fp}}{kT}\right)} \tag{3}$$

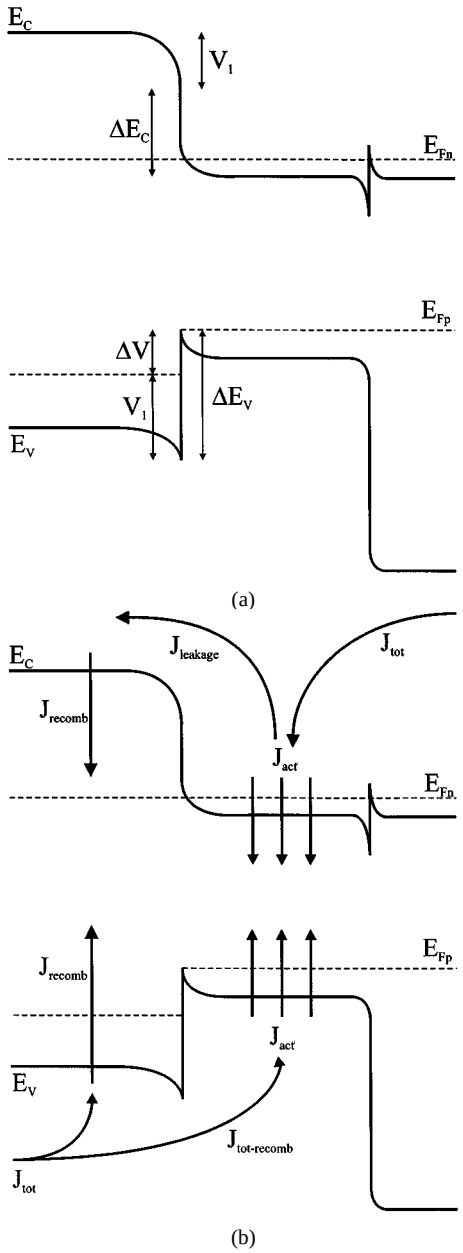

Fig. 1. (a) Schematic band structure of the laser. V_1 is the potential drop in the depletion layer, ΔE_v is the valence band discontinuity, and $q\Delta V$ is the change in hole quasi-Fermi level at the p-cladding to active region heterojunction. (b) Flow diagram of currents inside the laser. Since electron leakage dominates the total leakage flow, the current density of holes which reach the active region is the total amount of forward injected current $J_{\rm tot}$ minus the recombination current $J_{\rm recomb}$. $J_{\rm act}$, the current density injected into the active region, is the forward current which determines the degree of heterobarrier lowering as in [3] and (1) of this work.

(1) may be approximated by

$$\Delta V = R_{hj}J_{\rm act}. \tag{4}$$

We label this the **resistive regime** of the heterojunction $V-J$ characteristic. In (4), R_{hj} is given by

$$R_{hj} = \frac{kT}{q}\,\frac{L_D\exp\left(\dfrac{\Delta E_V - \Delta E_{Fn} - \Delta E_{Fp}}{kT}\right)}{\sqrt{2}\mu_p N_A\sqrt{qV_1kT}}. \tag{5}$$

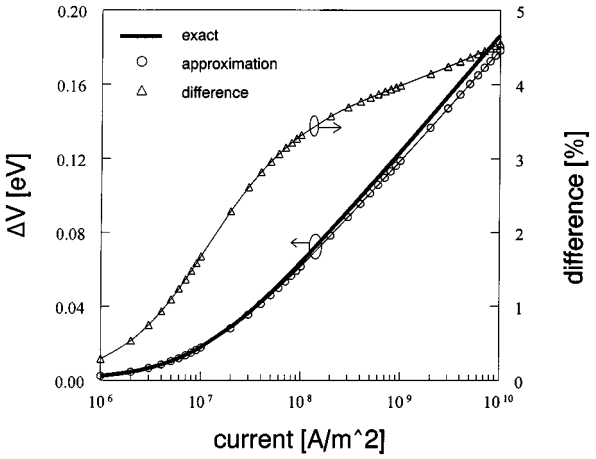

Fig. 2. ΔV as a function of current. The thick line denotes the exact value for ΔV, whereas the circles denote the approximation. The percentage difference between the exact and the approximate result is indicated with triangles. The approximate and exact values agree within 5%.

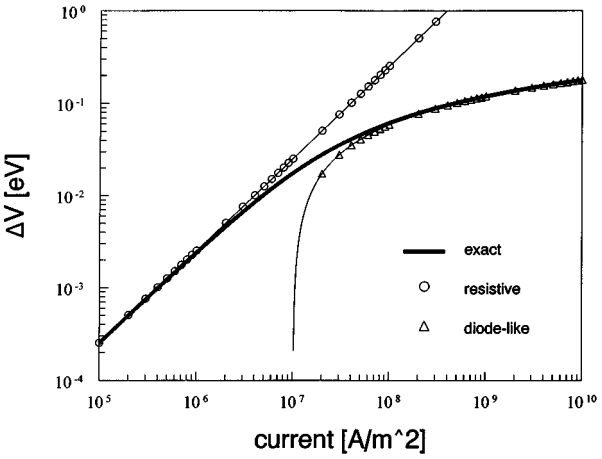

Fig. 3. Approximations and exact value of ΔV versus current. The thick line denotes the exact value for ΔV, and the circles and triangles denote, respectively, the approximations for the resistive and diode-like regimes. The transition current is: $J_{\text{transition}} = 1.1 \times 10^7$ A/m^2.

In comparison, for current densities substantially above the transition current density, the dependence of Fig. 2 corresponds to a **diode-like regime** of heterojunction behavior

$$J_{\text{act}}(V) = J_{hj0} \exp\left(\frac{q\Delta V}{kT}\right) \tag{6}$$

where

$$J_{hj0} = \frac{\sqrt{2}\mu_p N_A \sqrt{qV_1 kT}}{L_D \exp\left(\dfrac{\Delta E_V - \Delta E_{Fn} - \Delta E_{Fp}}{kT}\right)}. \tag{7}$$

In Fig. 3, we plot the exact value of ΔV for reference and plot the approximations of (4) and (6).

Whether the heterojunction V–J characteristic takes on a resistive or a diode-like character determines the qualitative and quantitative picture of overbarrier leakage. Considering drift and diffusive leakage of electrons into the p-cladding layer, we write [7], [8]

$$J_l = qD_n n_{\text{clad}} \cdot \left(\sqrt{\frac{1}{L_n^2} + \frac{1}{L_{nf}^2}} \coth \sqrt{\frac{1}{L_n^2} + \frac{1}{L_{nf}^2}} x_p + \frac{1}{L_{nf}}\right) \tag{8}$$

where x_p is the p-cladding layer thickness. In the limit of a p-contact, which is far in terms of minority carrier diffusion lengths from the active region, we may approximate (8) by

$$J_l = qD_n n_{\text{clad}} \left(\frac{1}{L_{nf}} + \sqrt{\frac{1}{L_n^2} + \frac{1}{L_{nf}^2}}\right). \tag{9}$$

Using Boltzmann's approximation, we may relate the leakage current out of the active region to the (known) carrier density within the active region

$$J_l = qD_n n_{\text{act}} \cdot \left(\frac{1}{L_{nf}} + \sqrt{\frac{1}{L_n^2} + \frac{1}{L_{nf}^2}}\right) \exp\left(-\frac{\Delta E_{\text{in,conf}} - \Delta V}{kT}\right) \tag{10}$$

where $\Delta E_{\text{in,conf}}$ is the initial confinement barrier at zero forward bias. We see that drift leakage is of the same magnitude as diffusive leakage when $L_n = L_{nf}$. We therefore define a transition current between diffusive dominated and drift dominated regimes

$$J_{l,\text{transition}} = 2\left(\frac{kT}{q}\right)\left(\frac{\sigma_p}{L_n}\right). \tag{11}$$

If the current is below this value, then diffusion will dominate and we can simplify (10) by discarding the L_{nf} influence

$$J_{l,\text{diffusive}} = \frac{qD_n n_{\text{act}}}{L_n} \exp\left(-\frac{\Delta E_{\text{in,conf}} - \Delta V}{kT}\right). \tag{12}$$

Above this transition current, drift will dominate:

$$J_{l,\text{drift}} = \frac{2qD_n n_{\text{act}}}{L_{nf}} \exp\left(-\frac{\Delta E_{in,conf} - \Delta V}{kT}\right). \tag{13}$$

In Fig. 4, we plot the exact value of J_l for reference and plot the approximations (12) and (13).

We are now able to apply the approximation for ΔV into the different regimes of the leakage model. In this particular case, we use the parameters for a laser operating at 1.55 μm at 350 K, also listed in Table I, which permits us to illustrate a case of great technological relevance. It is clear that one cannot use the resistive approximation for ΔV in the case of drift leakage, nor can one use the diode-like diffusive approximation when $J_{l,\text{transition}} < J_{\text{transition}}$.

Using (4) and (6) combined with (12) and (13), the four regimes can be expressed analytically as

$$\begin{aligned} J_{l,\text{resistive,diffusive}} &\propto \alpha \exp(\gamma J_{\text{act}}) \\ J_{l,\text{resistive,drift}} &\propto \beta J_{\text{act}} \exp(\gamma J_{\text{act}}) \\ J_{l,\text{diode-like,diffusive}} &\propto \alpha\gamma J_{\text{act}} \\ J_{l,\text{diode-like,drift}} &\propto \beta\gamma J_{\text{act}}^2 \end{aligned} \tag{14}$$

where α, β, and γ are independent of J_{act} (do depend on T, N_A, μ, etc.). In Fig. 5, we show the appropriate approximations when $J_{\text{transition}} < J_{l,\text{transition}}$ using (14).

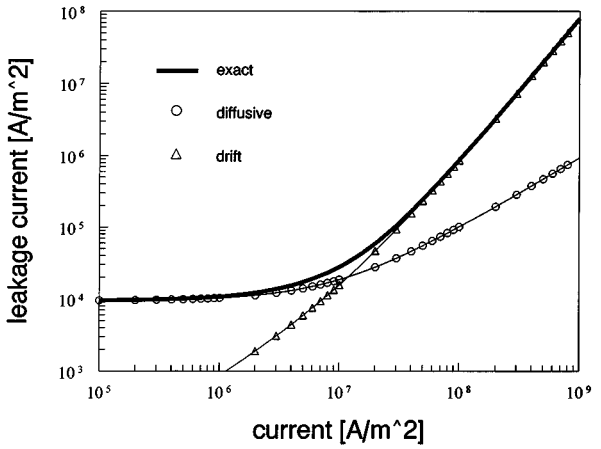

Fig. 4. Leakage current versus forward current. The thick line represents the exact leakage current using (10). Circles denote the diffusive approximation at currents below the transition current and triangles denote the drift approximation above the transition current. The transition current is: $J_{l,\text{transition}} = 2.3 \times 10^7$ A/m^2.

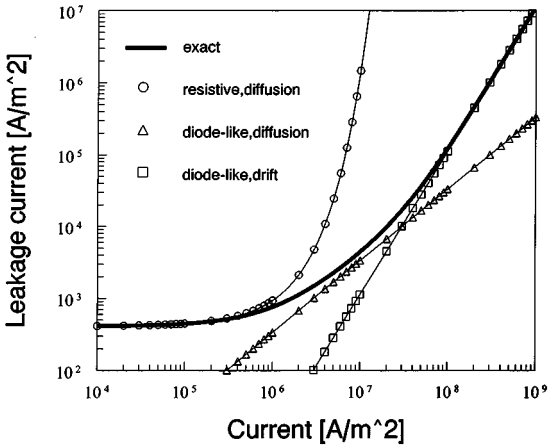

Fig. 5. Approximate leakage currents versus forward current. The thick line denotes the calculated leakage using (10). The open markers represents the approximations, respectively, from low to high current: the resistive/diffusive-, diode-like/diffusive-, and the diode-like/drift approximations.

It is apparent that the qualitative dependencies on forward current density differ markedly in the resistive and diode-like regimes. This has important implications as to the anticipated qualitative dependence of the light–current characteristic. We can write

$$P_{\text{out}} \propto J_{\text{act}} - J_{\text{th}} = J_{\text{tot}} - J_l - J_{\text{th}}. \tag{15}$$

As illustrated in Fig. 1(b), the internal efficiency η may be written

$$\frac{1}{\eta} = \frac{\partial J_{\text{tot}}}{\partial J_{\text{act}}} = 1 + \frac{\partial J_l}{\partial J_{\text{act}}}. \tag{16}$$

By using (16) on the four regimes in (14), we find for the internal efficiencies

$$\begin{aligned}
\eta_{\text{resistive,diffusive}} &= \frac{1}{1+\alpha\gamma\exp(\gamma J_{\text{act}})} \\
\eta_{\text{resistive,drift}} &= \frac{1}{1+\beta(1+\gamma J_{\text{act}}^2)\exp(\gamma J_{\text{act}})} \\
\eta_{\text{diode-like,diffusive}} &= \frac{1}{1+\alpha\gamma} \\
\eta_{\text{diode-like,drift}} &= \frac{1}{1+2\beta\gamma J_{\text{act}}}.
\end{aligned} \tag{17}$$

Knowing that typical threshold values are 1×10^7 A/m^2, we show in Fig. 6 the internal efficiency as a function of current. The bold line is calculated using the exact values for ΔV and (10). Using parameters for the 1.3-μm laser at 337 K, outlined in Table I, the transition currents are equal, $J_{\text{transition}} = J_{l,\text{transition}} = 2.3 \times 10^7$ A/m^2, just above threshold. This indicates that we should use the resistive/diffusive- and diode-like/drift approximations, the first and fourth equation from (17), respectively. Because the transition current is almost the same as the threshold current, the approximation for currents higher than threshold is well approximated by the diode-like/drift approximation, as can be seen in Fig. 6.

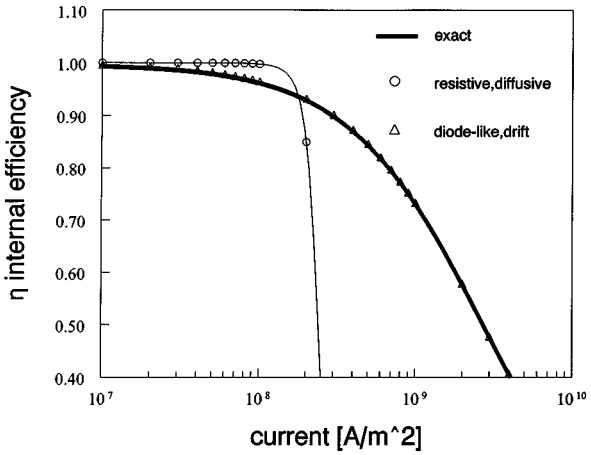

Fig. 6. Internal efficiency as a function of current. The thick line represents the exact value of the internal efficiency calculated using the exact value of ΔV and (10). Due to the fact that $J_{\text{transition}} = J_{l,\text{transition}}$, we are using the resistive/diffusive approximation, denoted by circles, and the diode-like/drift approximation denoted by triangles.

III. Consequences

In this section, we use our model to explore the effects of several physical laser parameters on the internal quantum efficiency within two devices, one designed for operation at 1.3 μm, the other at 1.55 μm. Both are assumed to be built in the InGaAsP-InP material system. We begin by using values from Table I and varying the temperature. Fig. 7 shows the efficiencies for both lasers at 300 and 400 K.

The results of Figs. 7 and 8 are for *internal* quantum efficiency, i.e., the net efficiency with which carriers are injected into the laser active region and participate in stimulated recombination. The *external* quantum efficiency of 1300-nm lasers is in fact typically higher than that of 1550-nm devices, predominantly a consequence of weaker inter-valence band absorption (IVBA) at shorter wavelengths [9].

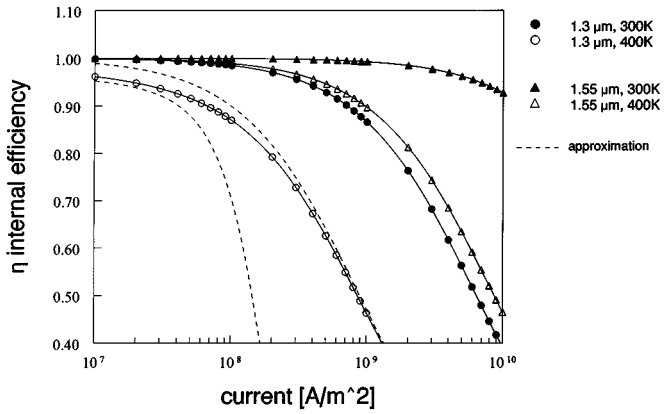

Fig. 7. Internal quantum efficiencies at 300 K (solid markers) and 400 K (open markers) for, respectively, a 1.3-μm laser (circles) and a 1.55-μm laser (triangles). Due to low transition currents $J \approx 1 \times 10^7$ A/m^2 in the 1.55-μm laser, the approximations at high currents, relative to the transition current, are equal to the exact value. Thus, we only need to make the approximation for the drift/diode-like regime. For the 1.3-μm laser, we need to make two approximations in the 400 K calculation. They are shown as dotted lines.

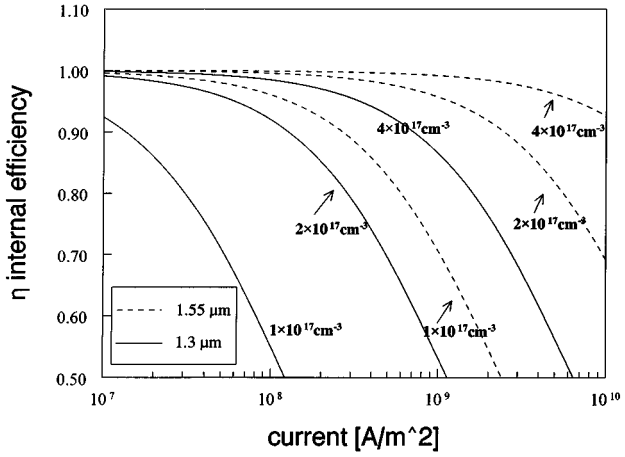

Fig. 8. Internal quantum efficiency versus current at different doping levels at 300 K. Solid lines denote the 1.3-μm laser, whereas dotted lines denote the 1.55-μm laser. The doping levels are 4×10^{17} cm^{-3}, 2×10^{17} cm^{-3}, and 10^{17} cm^{-3}. The approximations are made in the diode-like/drift regime. Due to low transition currents, the result of the approximation will be equal to the exact value.

The 1.3-μm laser is measurably degraded even at low current densities.

It is worth investigating the effect of doping at the heterojunction in both lasers. As mentioned in [2] and seen in (1), for higher N_A, ΔV increases more slowly with $J_{\rm act}$. By lowering the doping level, we will also decrease the initial confinement barrier height due to the fact that the Fermi level in the p-cladding will be farther into the bandgap away from the valence band edge compared to the higher doping case. Fig. 8 shows the effect of doping for both lasers.

It can be seen that the doping level adjacent to the active region is a very important material parameter to prevent overbarrier leakage. However, estimating a value for the doping level at the heterojunction is not trivial. It is difficult to know the exact doping profile of highly diffusive zinc which results from epitaxial growth. Zn is also known to rearrange within device lifetimes. As a result, caution is usually exercised in positioning the Zn doping front. It is therefore possible for the p-doping level over tens of nanometers, which define the p-cladding-to-active-region interface, to be much lower than the peak or average level throughout the InP p-contact. The 1.3-μm laser shows serious deleterious effects if the doping level is below 2×10^{17} cm^{-3}. Even in the much better confined 1.55-μm laser, the internal efficiency is merely 0.9 at 2×10^8 A/m^2. A 1.55-μm device operating with significant active region heating and modest doping at the depletion layer of 2×10^{17} cm^{-3} may thus suffer from severe degradation caused by overbarrier leakage.

IV. Conclusions

We have made a model for overbarrier leakage by approximating the behavior of a coupled self-consistent system over various regimes. We defined a transition current which separates two different regimes in the V–J heterojunction characteristic and treated the effects of drift and diffusive leakage of carriers through the depletion layer.

We have shown that, by using this analytical physical model for overbarrier leakage in a semiconductor laser, we can immediately see the influence of key parameters on lasing efficiency. We have shown that, in worst case scenarios, high temperatures and low doping levels, a 1.55-μm laser can exhibit a dramatic performance degradation as a result of overbarrier leakage.

Acknowledgment

The authors would like to thank J. K. Snel, E. C. F. Wong, and F. Chang for the many technical discussions and support.

References

[1] H. Watanabe *et al.*, "1.3-μm uncooled DFB lasers with low distortion for CATV application," *IEEE J. Select. Topics Quantum Electron.*, vol. 3, pp. 659–665, 1997.

[2] L. D. Westbrook and A. W. Nelson, "Electron leakage in 1.5-μm InGaAsP separate confinement heterostructure lasers," *J. Appl. Phys.*, vol. 56, pp. 699–704.

[3] R. F. Kazarinov and M. R. Pinto, "Carrier transport in laser heterostructures," *IEEE J. Quantum Electron.*, vol. 30, pp. 49–53, 1994.

[4] E. H. Sargent, G. Tan, and J. M. Xu, "Lateral current injection lasers: Underlying mechanisms and design for improved high-power efficiency," *J. Lightwave Technol.*, vol. 16, pp. 1854–1864, 1998.

[5] G. L. Belenky, D. V. Donetsky, C. L. Reynolds, R. F. Kazarinov, G. E. Shtengel, S. Luryi, and J. Lopata, "Temperature performance of 1.3-μm InGaAsP-InP lasers with different profile of p-doping," *IEEE Photon. Technol. Lett.*, vol. 9, pp. 1558–1560, 1997.

[6] P. K. Bhattacharya, *Properties of Lattice-Matched and Strained Indium Gallium Arsenide*. London, U.K.: INSPEC, 1993.

[7] D. P. Bour, D. W. Treat, R. L. Thornton, R. S. Geels, and D. F. Welch, "Drift leakage current in AlGaInP quantum-well lasers," *IEEE J. Quantum Electron.*, vol. 29, pp. 1337–1343, 1993.

[8] G. P. Agrawal and N. K. Dutta, *Long Wavelength Semiconductor Lasers*. New York, NY: Van Nostrand Reinhold, 1986.

[9] G. N. Childs, S. Brand, and R. A. Abram, "Intervalence band absorption in semiconductor laser materials," *Semicond. Sci. Technol.*, vol. 1, pp. 116–120, 1986.

Igor M. P. Aarts was born on February 26, 1976. He is currently working toward the M.S. degree in applied physics at the Eindhoven University of Technology, Eindhoven, The Netherlands.

As an exchange student, he visited the group of Prof. Sargent at the University of Toronto. His supervisor at the Eindhoven University of Technology is Prof. J. H. Wolter, the scientific director of COBRA, the Inter-University Research Institute on Communication Technology Basic Research and Applications.

Edward H. Sargent holds the Nortel Junior Chair in Emerging Technologies in the Department of Electrical and Computer Engineering at the University of Toronto, Toronto, ON, Canada. He leads a group of 12 graduate and post-doctoral researchers in the areas of semiconductor quantum electronic devices, photonic crystal applications, hybrid organic–inorganic quantum dot electroluminescence, and multiple-access optical networks.

Prof. Sargent was awarded the Silver Medal of the Natural Sciences and Engineering Research Council of Canada in 1999 for his work on the lateral current injection lasers. Also, in 1999, he won the Premier's Research Excellence Award in recognition of research into the application of photonic crystals in lightwave systems.